Non-Uniform Waveband Hierarchy in Hybrid Optical Networks

Rauf Izmailov Samrat Ganguly Viktor Kleptsyn* Aikaterini C. Varsou

NEC Laboratories America, Inc.
4 Independence Way
Princeton, NJ 08540

***Abstract*— Aggregation of individual wavelengths into wavebands for their subsequent switching and routing as a single group is an attractive way for scalable and cost-efficient optical networks. We analyze the implications of this waveband hierarchy for a single optical node by analyzing two issues: the proper selection of waveband sizes and the assignment of wavebands for a limited set of input-output patterns of traffic. We formulate a general model and propose optimal algorithmic solutions for both problems. The performance of resulting sets of non-uniform wavebands is studied for several representative cases (a single node, an optical ring network, an optical mesh network). The results demonstrate improved optical throughput and reduced cost of switching and routing when using non-uniform waveband hierarchy.**

I. Introduction

The continuing increase of data traffic keeps the pressure on the backbone telecommunication networks requiring more diverse and more intelligent allocation of capacity. Optical networking has become a key technology in accommodating the rapidly expanding Internet traffic. New optical networks are expected to support the increasing network load by employing both sophisticated transmission (wavelength division multiplexing division (WDM)) and switching technologies (optical switches and cross-connects) [1]. While WDM technology increases the transmission capacity of fiber links by two-to-three orders of magnitude, it comes at the expense of managing the wavelengths (separating, combining, adding, dropping, routing, switching, and converting), which have to be handled by the switching equipments. Switching is thus becoming a cost-performance bottleneck.

In IP networks, concerns about performance and scalability of switching prompted the development of layered mechanisms that provide various levels of traffic aggregation supported by DiffServ [2] and MPLS standards [3]. In the case of optical networking, the same cost and scalability concerns translate into creation of multiple switching granularities, such as wavelengths and wavebands [4], [5]. The optical paths thus form a hierarchy, in which a higher-layer path (waveband) consists of several lower layer paths (wavelengths). The potential cost benefits of wavelength aggregation into wavebands was demonstrated in [6] and further analyzed in [7]. A waveband path occupies only two (input and output) ports of an optical switch in a node. Path hierarchy reduces node costs since a waveband can be switched optically as a single unit, thus reducing the number of expensive optical-electrical-optical (OEO) ports that are required for processing individual wavelengths.

Cost-efficient implementation of optical hierarchy has to be delivered by appropriately designed routing, aggregation and assignment algorithms. Routing and wavelength assignment algorithms were extensively studied in the general context of optical networking ([1] and its references). The organization of wavelengths into wavebands can be further improved by using non-uniform wavebands (containing different number of wavelengths), as proposed in [8], [9]. Non-uniform wavebands provide more flexibility for wavelength aggregation, which can be used for more efficient switching and routing mechanisms [10].

The paper is organized in the following way. In the next section, we provide a general background for the problem. In Section III, we formalize the model and formulate two problems of waveband hierarchy: the proper selection of waveband sizes and the assignment of wavebands for a limited set of input-output patterns of traffic. We further propose optimal algorithmic solutions for both problems in the same section. We then explore the node-level and network-level performance of non-uniform wavebands (for ring and mesh networks) in Sections V and VI respectively. Finally, we conclude the paper with an outline of future work.

II. Problem Background

Emerging hybrid hierarchical optical cross-connects [11], [12] may become an attractive solution for next generation optical networks due to reduction in the switching cost. On the node level, these systems combine the flexible non-uniform wavebands with two promising technologies: a hybrid of all-optical (OOO) and optical-electronic-optical (OEO) cross-connects and the hierarchical processing of wavelengths aggregated into wavebands. On the network level, they provide

*V. Kleptsyn is with Moscow State University and Independent University of Moscow, Moscow, Russia.

diverse provisioning and protection of various types of traffic. In the next three subsections, these key components are described in more detail.

A. Hybrid Technology

Currently, optical networks are at the stage of circuit switching. The circuits in optical networks are being handled by optical add-drop multiplexers (OADMs) and optical cross-connects (OXCs). These critical network elements sit at junction points in optical backbones and enable carriers to string together wavelengths in order to provide end-to-end connections. Over the last few years, the equipment vendors have been developing two distinct and competing versions of cross-connects: OEO (opaque) and all-optical (transparent). OEO-based cross-connects (XC) convert the incoming optical signal into electrical signal for subsequent switching and grooming; the electrical signal is regenerated as a new optical signal at the output port. OEO-based XCs are based on mature and reliable technology. They can provide a variety of functions such as optical 3R (regeneration, reshaping, retiming), grooming and wavelength conversion. However, these rich functionalities need to be supported by expensive hardware, which, being protocol-dependent and bit-rate dependent, cannot scale well. OEO-based XCs are also characterized by large footprint and large power consumption, generating significant amount of heat.

In contrast, an all-optical XC transparently switches the incoming optical signal through the switching fabric where the optical signal remains in optical domain when it emerges from an output port. A variety of technologies can be used for the switching fabric like MEMS, liquid crystal, planar lightwave circuit, electrohologram. All-optical XCs are less expensive than OEO-based XCs: they have a smaller footprint, consume less power and generate less heat. However, the absence of optical 3R functions (required to clean up accumulated optical impairments) and wavelength conversion (required to resolve wavelength contention) restricts the capabilities of pure all-optical XCs. The absence of signal visibility makes it harder to monitor performance in all-optical XC. All-optical XCs have the advantage of being highly scalable: multiple wavelengths can be handled using the same port. Being naturally protocol-independent and bit-rate independent, they are able to carry services in their native format, providing a future-proof alternative for OEO-based systems.

The hybrid technology (employing both types of cross-connects, OEO and all-optical) is emerging [13] as an inevitable convergence point leveraging the advantages of both technologies (Figure 1). Since optical networks are dominated by rapidly growing long-distance data traffic, most of the traffic passing through the optical nodes (as much as 75% percent) consists of transit traffic. A hybrid cross-connect can use the all-optical component to route the transit traffic while the OEO component is used for aggregating and adding the local traffic. Electronics is thus used to perform necessary and

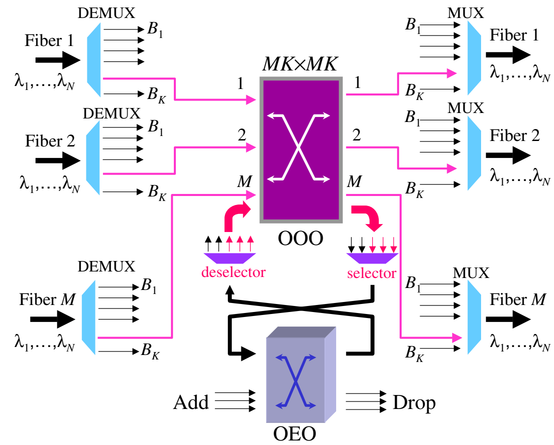

Fig. 1. Hybrid hierarchical cross-connect node.

expensive processing of the traffic, while optics is used for inexpensive and transparent forwarding. Merging the best of both technologies, the resulting single platform for supporting all-optical and OEO fabrics can be managed as a single integrated unit, further improving the performance.

Figure 1 illustrates a general architecture of a hybrid OXC with M input and M output fibers, each carrying N wavelengths, $\lambda_1, \ldots, \lambda_N$. Most of the incoming wavelengths are being switched by the all-optical (OOO) part of the hybrid, while the OEO part of the hybrid handles add/drop traffic along with contention resolution and signal regeneration.

B. Hierarchical Technology

As already mentioned, cost and scalability concerns in optical networks leads to the creation of multiple switching granularities, such as wavelengths and wavebands. Standard routing protocols cause many traffic flows to run alongside each other over the same path of links. This creates an opportunity to aggregate express optical wavelengths into wavebands (also called "fat pipes" or "super channels") that can be optically (transparently) switched through the network for the most part of their path, without being demultiplexed into separate wavelengths at every node. The optical paths thus form a hierarchy in which higher-layer paths (wavebands) consist of several segments of lower-layer paths (wavelengths). The resulting hierarchy of wavelengths and wavebands is a mixed one: logical wavebands coexist with individual wavelengths on the same fiber, thus providing better efficiency. The potential cost benefits of wavelength aggregation into wavebands were demonstrated in literature [4], [6], [14], [15]. Furthermore, the hierarchical technology is emerging as one of the key solutions for the looming scalability problem of optical networks. All-optical XCs (or the all-optical part of hybrid XCs) can switch large wavebands rather than individual wavelengths, without any extra cost (as opposed to OEO-based XCs that are bit-rate-dependent).

Treating multiple wavelengths within a waveband as a single unit reduces the size and complexity of the optical switching

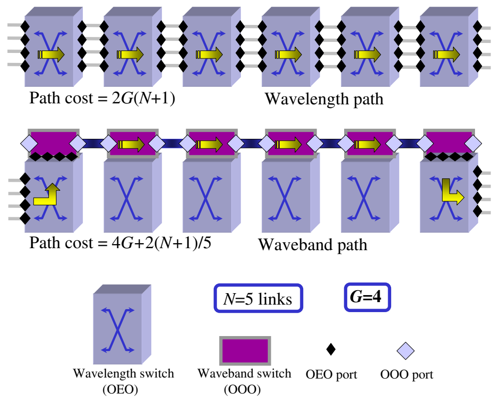

Fig. 2. Routing metric: wavelengths and wavebands.

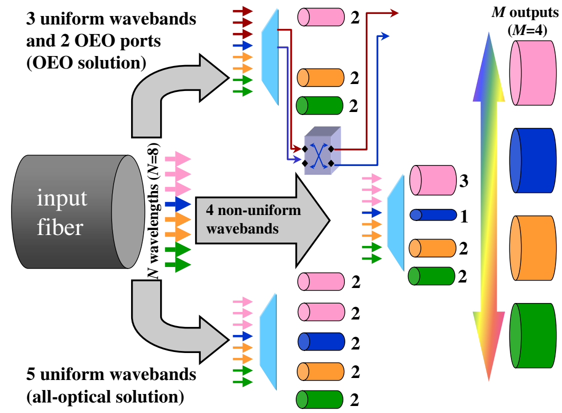

Fig. 3. Example of uniform and non-uniform wavebands.

matrices. In addition, optical amplifiers can operate on an entire waveband without any knowledge of the individual wavelengths. Hierarchical OXC also cuts costs in DWDM mux-demux and transmit-receive subsystems that are used before the input and after the output of the cross-connect.

In Figure 1, the incoming traffic of each fiber is being split into K wavebands, which are then being switched by the OOO. Since $K < N$, this arrangement reduces the size of the all-optical part of the switch.

To quantify the advantages of hierarchical technology, we assume that some of the wavelengths can be aggregated into wavebands consisting of G wavelengths each (Figure 2). Each waveband consists of contiguous wavelengths*, i.e. the mth waveband contains all the wavelengths with numbers from $(m-1)G+1$ to mG . We define the cost of routing in hierarchical optical network as the total cost of the ports (both OEO and OOO ones) required for routing the traffic flows. For this we assume an optical port costs five times less than an OEO port, which is the unit of cost. Thus the cost of a wavelength segment consisting of N links is equal to $2G(N+1)$, while the cost of a waveband segment aggregating this wavelength segment is equal to $4G+2(N+2)/5$. Figure 2 illustrates the cost computation for a wavelength segment consisting of $N = 5$ links and for granularity $G = 4$. Cost-efficient implementation of optical hierarchy has to be delivered by appropriately designed routing and aggregation algorithms [7]. While routing and wavelength assignment algorithms have been studied extensively in the general context of optical networking ([1] and its references), the hierarchical approach adds another layer: appropriate routing, wavelength and waveband assignment algorithms are needed.

C. Non-Uniform Wavebands and Waveband Deaggregator

The aggregation of wavelengths into uniform wavebands (each comprised of G wavelengths) introduces aggregation overhead, which is adversely affecting the performance of hierarchical nodes as discussed next. Furthermore, with the deaggregator being fixed, uniform wavebands cannot properly aggregate a varying traffic scenario.

Consider an optical switching node with M output fibers and suppose that the input fiber carries N wavelengths to be switched to any of M outputs. Depending on the breakdown of wavelengths among the output fibers, the efficiency of their aggregation into wavebands may vary. Consider the example in Figure 3. It shows an input fiber carrying $N = 8$ wavelengths that have to be switched into $M = 4$ output fibers (shown as four pipes in the right side of Figure 3). The numbers of wavelengths to be switched to the four output fibers are equal to (3,1,2,2). In Figure 3, the wavelengths to be switched to the same output fiber are painted in the same color as that of the output fiber; for example, the upper three “light” wavelengths are to be switched to the uppermost “light” output, one “dark” wavelength is to be switched to the “dark” output just below the uppermost “light” output, etc. We assume that the waveband granularity $G = 2$: the wavelengths can be aggregated into preconfigured uniform wavebands of the size of two wavelengths each. In this example, two switching solutions can be employed. In the first approach (*OEO solution*, shown in the upper part or Figure 3), two expensive OEO ports are used to switch two of the wavelengths in the OEO layer, while three wavebands are used to switch the remaining wavelengths. In the second approach (*all-optical solution*, shown in the lower part of Figure 3), five wavebands are used to switch all the traffic in the all-optical domain.

However, the same wavelength demand (3,1,2,2) could have been switched optically if the wavebands had been preconfigured in the way shown as *non-uniform solution* (shown in the middle part of Figure 3): two wavebands containing two wavelengths each, one waveband containing three wavelengths and one waveband containing one wavelength.

Figure 4 illustrates all breakdowns of $N = 8$ wavelengths between $M = 2$ output fibers and the equipment costs required to carry those wavelengths (for uniform and non-uniform wavebands). Depending on the particular approach, uniform wavebands approach requires up to five wavebands (all-optical solution) or three wavebands and two OEO ports

*In general, the wavelengths do not need to be contiguous.

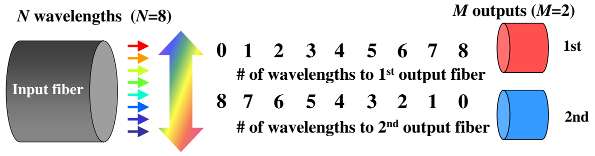

wavelengths directed to 1st fiber	2nd fiber	uniform wavebands $2\lambda + 2\lambda + 2\lambda + 2\lambda$ 1st fiber	2nd fiber	All-optical cost	OEO cost	non-uniform wavebands $1\lambda + 1\lambda + 2\lambda + 4\lambda$ 1st fiber	2nd fiber	cost
0	8	0	2+2+2+2	4wb	4wb	0	1+1+2+4	4wb
1	7	2	2+2+2+2	5wb	3wb+2oeo	1	1+2+4	4wb
2	6	2	2+2+2	4wb	4wb	2	1+1+4	4wb
3	5	2+2	2+2+2	5wb	3wb+2oeo	1+2	1+4	4wb
4	4	2+2	2+2	4wb	4wb	4	1+1+2	4wb
5	3	2+2+2	2+2	5wb	3wb+2oeo	1+4	1+2	4wb
6	2	2+2+2	2	4wb	4wb	1+1+4	2	4wb
7	1	2+2+2+2	2	5wb	3wb+2oeo	1+2+4	1	4wb
8	0	2+2+2+2	0	4wb	4wb	1+1+2+4	0	4wb

Fig. 4. Switching costs of uniform and non-uniform wavebands (2 output fibers, 8 wavelengths).

(OEO solution) to carry all possible traffic loads, whereas the approach based on non-uniform wavebands consistently requires only four wavebands for all traffic distributions.

This example gives rise to the following two issues. The first one is how to preconfigure a minimum set of wavebands that can be used to represent an arbitrary breakdown of input flow of N wavelengths into M output fibers. We call it *the waveband selection problem*. The second issue is how to assign these preconfigured wavebands for optical switching of N wavelengths into M output fibers. We call it *the waveband assignment problem*. Both problems are formally defined and solved in the sequel.

In the next section, we will concentrate on the waveband selection and waveband assignment problems. Both can be formally defined in the context of partition theory. We will therefore start with standard definitions related to set partition, which we will then use in order to formulate a description of these problems. To the best of our knowledge, the current work is the first to formulate and solve the above problems. It is related to certain well-known problems [16] such as postage-stamp problem, knapsack problem, and change-making problem. The closest one is the k-payment problem [17], which was motivated by electronic cash model, where exact representation of each payment by the corresponding set of coins is required. Our problem, in contrast, is motivated by optical switching, where the hardware cost depends on the size of switching matrix, while the switched wavebands (coins) may or may not be completely occupied by wavelengths (units) unlike the k-payment problem. As a result, our problem requires its own solution as it will be discussed next.

III. Formal Model and Main Results

Definition 1. An *ordered sequence* is a list of integers $\{v_1, v_2, \ldots, v_M\}$, where $0 \leq v_1 \leq v_2 \leq \ldots \leq v_M$.

Definition 2. An *(N, M)-partition* is a sequence $\{v_1, v_2, \ldots, v_M\}$, where $v_1 + v_2 + \ldots + v_M = N$. If $\{v_1, v_2, \ldots, v_M\}$ is an ordered sequence, the partition is *ordered*.

Example. The ordered sequence $\{1, 1, 2, 4, 5\}$ is an ordered $(13, 5)$-partition. More details on partitions are contained in [18] and its references.

Definition 3. An ordered (N, K)-partition $B = \{b_1, b_2, \ldots, b_K\}$ *covers* the (N, M)-partition $V = \{v_1, v_2, \ldots, v_M\}$ if B can be partitioned into M disjoint sub-sequences $\{b_1^1, b_2^1, \ldots, b_{p_1}^1\}$, $\{b_1^2, b_2^2, \ldots, b_{p_2}^2\}$, …, $\{b_1^M, b_2^M, \ldots, b_{p_M}^M\}$, where $p_1 + p_2 + \ldots + p_M = K$ and

$$\begin{cases} v_1 = b_1^1 + b_2^1 + \ldots + b_{p_1}^1, \\ v_2 = b_1^2 + b_2^2 + \ldots + b_{p_2}^2, \\ \vdots \\ v_M = b_1^M + b_2^M + \ldots + b_{p_M}^M. \end{cases}$$

Example. The $(20, 6)$-partition $\{1, 1, 2, 4, 5, 7\}$ covers the $(20, 3)$-partition $\{2, 7, 11\}$ since

$$11 = 7 + 4, \; 7 = 5 + 2, \; 2 = 1 + 1.$$

Definition 4. An *(N, M)-cover* is an ordered partition that covers all (N, M)-partitions.

Example. The $(6, 3)$-partition $B = \{1, 2, 3\}$ is a $(6, 2)$-cover, since all ordered $(6, 2)$-partitions can be covered by B in the following way:

$$\begin{cases} \{0, 6\} & \text{is covered as} & 6 = 3 + 2 + 1 \\ \{1, 5\} & \text{is covered as} & 1 = 1, \; 5 = 3 + 2 \\ \{2, 4\} & \text{is covered as} & 2 = 2, \; 4 = 3 + 1 \\ \{3, 3\} & \text{is covered as} & 3 = 2 + 1, \; 3 = 3. \end{cases} \tag{1}$$

Definition 5. An (N, k)-partition that is an (N, M)-cover is called an *(N, M, k)-cover* and is denoted by $B(N, M, k)$.

Example. The already mentioned $(6, 3)$-partition $B = \{1, 2, 3\}$ is a $(6, 2, 3)$-cover.

Optimization problem. Given N and M, find the minimum k such that there exists an (N, M, k)-cover.

Example. As (1) demonstrates, $k \leq 3$, since there exists a $(6, 2, 3)$-cover $B = \{1, 2, 3\}$. On the other hand, $k > 2$, since no ordered $(6, 2)$-partition $B = \{a, 6 - a\}$ can cover all $(6, 2)$-sequences (for instance, the ordered sequence $\{a, 6 - a\}$, where $a < 6$, cannot cover the $(6, 2)$-sequence $\{a + 1, 6 - a - 1\}$). Therefore, $k(6, 2) = 3$.

Assignment problem. Given an (N, M)-partition $V = \{v_1, v_2, \ldots, v_M\}$ and $B(N, M, k) = \{b_1, b_2, \ldots, b_k\}$, find the partition of $B(N, M, k)$ into M disjoint sub-sequences $\{b_1^1, b_2^1, \ldots, b_{p_1}^1\}$, …, $\{b_1^M, b_2^M, \ldots, b_{p_M}^M\}$, where $p_1 + p_2 + \ldots + p_M = k$ and

$$\begin{cases} v_1 = b_1^1 + b_2^1 + \ldots + b_{p_1}^1, \\ v_2 = b_1^2 + b_2^2 + \ldots + b_{p_2}^2, \\ \vdots \\ v_M = b_1^M + b_2^M + \ldots + b_{p_M}^M. \end{cases}$$

For example, (1) shows the solution of the assignment problem for the $(6, 2, 3)$-cover $B = \{1, 2, 3\}$ and any ordered $(6, 2)$-partition V.

The solutions of the optimization and assignment problems are presented in the next two subsections.

A. Optimization Problem

Lemma 1. The smallest $M-1$ elements b_j of any (N,M,k)-cover $B(N,M,k)$ are equal to 1, i.e.,

$$b_j = 1, \text{ where } j = 1, ..., M-1.$$

Proof of Lemma 1. Consider the (N,M)-partition $V = \{1, ..., 1, N-M-1\}$, where $v_j = 1$, for all $j = 1, \ldots, M-1$. These $M-1$ values v_j can only be covered by the elements of $B(N,M,k)$ that are equal to 1. This proves Lemma 1.

Lemma 2. The largest element b_k of (N,M,k)-cover $B(N,M,k)$ satisfies the inequality $b_k \leq \lceil N/M \rceil$.

Proof of Lemma 2. Let $N/M = \lfloor N/M \rfloor + r/M$, where $0 \leq r \leq (M-1)$. Then $\lceil N/M \rceil = N/M + (M-r)/M$. Therefore, we can construct the (N,M)-partition $V = \{v_1, \ldots, v_M\}$, where $v_1 = \ldots = v_{M-r} = \lfloor N/M \rfloor$ and $v_{M-r+1} = \ldots = v_M = \lceil N/M \rceil$. This partition cannot be covered by any (N,M,k)-cover B if any of its elements b_k is larger than $\lceil N/M \rceil$. This proves Lemma 2.

Lemma 3. The largest element v_M in any ordered (N,M)-partition $V = \{v_1, \ldots, v_M\}$ satisfies the inequality $v_M \geq \lceil N/M \rceil$.

Proof of Lemma 3. Since v_M is the largest element, $v_1 + \ldots + \ldots + v_M \leq M v_M$. If $v_M < \lceil N/M \rceil$ then $M v_M < N$ and the sequence $\{v_1, \ldots, v_M\}$ cannot sum to N. This proves Lemma 3.

Lemma 4. Let s_p be the sum of the first p elements of an (N,M,k)-cover $B = \{b_1, \ldots, b_k\}$: $s_p = b_1 + \ldots + b_p$. Then $s_p \geq (M-1)(b_{p+1}-1)$, for any $p \geq M-1$.

Proof of Lemma 4. Suppose that this inequality does not hold for some p i.e.,

$$s_p < (M-1)(b_{p+1}-1). \tag{2}$$

Consider the partition $\{b_{p+1}-1,\ b_{p+1}-1, ...,\ b_{p+1}-1,\ N-(M-1)(b_{p+1}-1)\}$. None of the last elements b_i of $B(N,M,k)$ with $i > p$ can be used for covering the first $M-1$ elements of the partition (since they all are larger than b_{p+1}). However, the sum of the first $M-1$ elements is $(M-1)(b_{p+1}-1)$ and, by assumption 2, the first p elements of $B(N,M,k)$ are insufficient to cover the sum. Therefore, the sequence $B(N,M,k)$ is not a cover, which contradicts the definition of $B(N,M,k)$. Lemma 4 is therefore proven.

Now consider an ordered sequence $C = \{c_1, c_2, \ldots, c_r\}$, which is an (N,M)-cover. According to Lemma 1, $c_1 = ... = c_{M-1} = 1$. From Lemma 4, $s_p \geq (M-1)(c_{p+1}-1)$, for any $p \geq M-1$. Therefore, $c_{p+1} \leq 1 + s_p/(M-1)$. Since $s_{p+1} \equiv s_p + c_{p+1} \leq s_p + 1 + s_p/(M-1)$, we have

$$s_p \geq \frac{(M-1)(s_{p+1}-1)}{M}.$$

Since s_p are integers, we can write

$$s_p \geq \left\lceil \frac{(M-1)(s_{p+1}-1)}{M} \right\rceil. \tag{3}$$

We proceed with the following theorem.

Theorem 1. An optimal (N,M)-cover can be generated by selecting the maximum of all s to be equal to N and assigning s_p for all $p \geq M-1$ using the recursive formula

$$s_p = \left\lceil \frac{(M-1)(s_{p+1}-1)}{M} \right\rceil. \tag{4}$$

Proof of Theorem 1. Consider two sequences $S^c = \{s^c_M, s^c_{M-1}, \ldots\}$ and $S^b = \{s^b_M, s^b_{M-1}, \ldots\}$, with their first elements $s^c_M = s^b_M = N$ and the other elements generated by sequential application of inequality (3) and equality (4), respectively. Suppose that

$$s^c_m \leq s^b_m, \quad \text{for all } m. \tag{5}$$

Then the sequence S^c cannot have less elements than S^b. The same is true for the corresponding sequences $C = \{c_M, c_{M-1}, \ldots\}$ and $B = \{b_M, b_{M-1}, \ldots\}$ generated by the differences $c_j = s^c_j - s^c_{j-1}$ and $b_j = s^b_j - s^b_{j-1}$ of adjacent elements in S^c and S^b: the sequence C cannot have less elements than B. Therefore, in order to prove optimality of B, it is sufficient to prove (5).

If $S^c = S^b$, then (5) holds and Theorem 1 is proven. Suppose that S^c and S^b are different and (5) is not true. Consider the smallest j for which $s^c_j < s^b_j$. By definition of j, $s^c_{j+1} = s^b_{j+1} + \Delta$ where $\Delta \geq 1$. From equation (4) and inequality (3), we have

$$\begin{cases} s^b_j = \dfrac{(M-1)(s^b_{j+1}-1)}{M} + \delta^b; & \delta^b \in [0,1). \\ s^c_j = \dfrac{(M-1)(s^c_{j+1}-1)}{M} + \delta^c; & \delta^c \geq 0. \end{cases} \tag{6}$$

Subtracting the first line from the second one and substituting $s^c_{j+1} = s^b_{j+1} + \Delta$, we have

$$s^c_j - s^b_j = \frac{(M-1)\Delta}{M} + \delta^c - \delta^b.$$

Since $(M-1)\Delta/M > 0$ and $\delta^c - \delta^b > -1$, the inequality $s^c_j - s^b_j > -1$ holds. Since $s^c_j - s^b_j$ is an integer, $s^c_j - s^b_j \geq 0$, which contradicts the assumption $s^c_j < s^b_j$. Theorem 1 is then proven.

Let the sequence of k numbers $C = \{c_1, \ldots, c_k\}$ be an optimal (N,M)-cover. By the sum definition of Lemma 4, $s_k = N$. From inequality (3), we have

$$s_{k-1} \geq \frac{(M-1)(N-1)}{M},$$

which means that

$$c_k = s_k - s_{k-1} \leq N - \frac{(M-1)(N-1)}{M} = \frac{N+M-1}{M}.$$

Since c_k is an integer, this inequality is equivalent to $c_k \leq \lceil N/M \rceil$. By Theorem 1, an optimal cover is generated by selecting the equality at this point, so $c_k = \lceil N/M \rceil$. Denoting $N' = N - c_k = s_{k-1}$, we can proceed with the next element of C as $c_{k-1} = (N' + M - 1)/N'$. Therefore, sequential application of equality (4) in Theorem 1 generates an optimal cover.

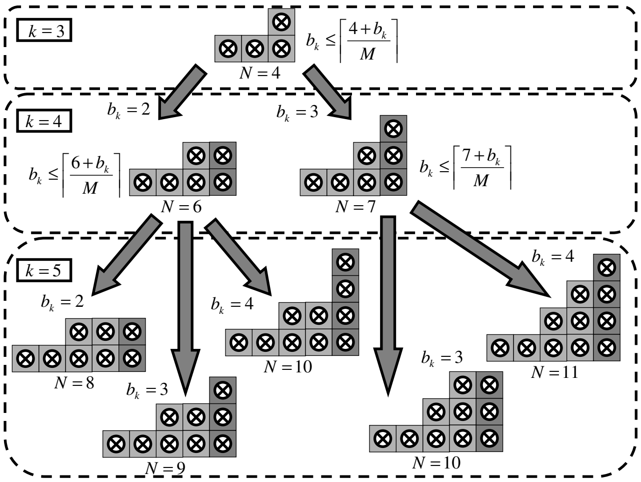

Fig. 5. Construction of regular covers.

Formally, the optimal cover B can be constructed using the following algorithm.

Algorithm 1. Waveband Cover Construction (WCC).

1) Input the parameters N and M.
2) Create the set $B = \{\emptyset\}$.
3) Assign $N' = \lceil N/M \rceil$.
4) Add the element N' to the set B.
5) Assign $N = N - N'$.
6) If $N = 0$, stop. Else go to step 3.

B. Assignment Problem

Theorem 2. The (N, M, k)-cover $B(N, M, k) = \{b_1, \ldots, b_k\}$ can be generated from a smaller $(N - b_k, M, k - 1)]$-cover $B(N - b_k, M, k - 1)$ as $B(N, M, k) = \{B(N - b_k, M, k - 1), b_k\}$ where $b_k \le \lceil N/M \rceil$.

Proof of Theorem 2. We have to prove that any ordered (N, M)-partition $V = \{v_1, v_2, \ldots, v_M\}$ can be covered by $B(N, M, k)$. By Lemma 3, $v_M \ge \lceil N/M \rceil$, so we can assign b_k to the v_M. This generates $v'_M = v_M - b_k < v_M$ and the new sequence $V' = \{v_1, v_2, \ldots, v_{M-1}, v'_M\}$, which sums to $N - b_k$. By the definition of covers, $B(N - b_k, M, k - 1)$ covers V'. This proves Theorem 2.

Definition 6. A cover $B(N, M, k) = \{b_1, \ldots, b_k\}$ is *regular* if all its subsequences $\{b_1, \ldots, b_j\}$, $j < k$, are recursively generated using Theorem 2.

Figure 5 illustrates the construction of regular covers starting from the (4,3)-cover $B = \{1, 1, 2\}$ using Ferrer's diagrams [18]. At each step k, the current (N, M)-cover $\{b_1, \ldots, b_{k-1}\}$ can be augmented by a new element $b_k \ge b_{k-1}$, where $b_k \le \lceil (N + b_k)/M \rceil$.

The optimal cover generated by the Waveband Cover Construction algorithm is regular. According to Theorem 2, all sub-sequences $\{b_1, \ldots, b_j\}$ of a regular cover $B(N, M, k)$ are $(N - \sum_{j+1}^{k} v_i, M, j)$-covers. This means that the largest element b_{j+1} of the cover can be assigned to any element v_i of $V = \{v_1, \ldots, v_M\}$, in which it fits (i.e., $b_{j+1} \le v_i$) and the solution of assignment problem is guaranteed. Note that the elements b_j have to be assigned in descending order, as there is no guarantee that an arbitrary sub-sequence of $B(N, M, k)$ is a cover.

element of cover B	v_1 v_2 v_3	assignment
$b_1 = 3$	5 3 1	$b_1 \to v_1$
$b_2 = 2$	2 3 1	$b_2 \to v_2$
$b_3 = 2$	2 1 1	$b_3 \to v_1$
$b_4 = 1$	0 1 1	$b_4 \to v_1$
$b_5 = 1$	0 0 1	$b_5 \to v_3$

TABLE I
ASSIGNMENT OF $B(9, 3, 5) = \{3, 2, 2, 1, 1\}$ TO $\{5, 3, 1\}$.

The assignment can be performed using a sorted binary heap structure as follows. Assume that the values b_j in $B(N, M, k)$, where $j = 1, \ldots, k$, are stored in descending order. The input (N, M)-partition $V = \{v_1, v_2, \ldots, v_M\}$ is stored as a heap, something that requires $O(M)$ time for heap construction. At the j^{th} step of assignment, the following steps are taken.

Algorithm 2. Waveband Cover Assignment (WCA).

1) The topmost element V_t of the heap is deleted from the heap.
2) The element b_j is assigned to V_t.
3) The element $V_t - b_j$, if it is non-zero, is inserted into the heap.

The j^{th} step that includes a deletion and an insertion to the heap requires $O(\log_2 M)$ time. Since these steps are carried k times in order to assign all b_j for $j = 1, \ldots, k$, the overall assignment can be completed in $O(k \log_2 M)$ time.

Example. Consider the cover $(9, 3, 5)$-cover $B = \{b_1, \ldots, b_5\} = \{3, 2, 2, 1, 1\}$. The assignment for the $(9, 3)$-partition $\{v_1, v_2, v_3\} = \{5, 3, 1\}$ is demonstrated in Table I. Each row of the table shows the assignment of b_j to the largest element v_i of the remaining elements $\{v_1, v_2, v_3\}$ and the resulting update of v_i as $v_i = v_i - b_j$.

Note that the elements b_j of the cover are assigned in descending order of their values. If they were assigned in the order $b_2 \to v_1$, $b_3 \to v_1$, $b_4 \to v_1$, $b_5 \to v_2$, the last element $v_1 = 3$ could not be used to cover the remaining elements $\{v_1, v_2, v_3\} = \{1, 1, 1\}$.

IV. NON-UNIFORM WAVEBAND DE-AGGREGATOR AND IMPLEMENTATION RESTRICTIONS

Non-uniform optical wavebands can be realized by a waveband (de)aggregator subsystem that can realize and process non-uniform wavebands.

In order to maintain the best optical performance, the preferred way to separate waveband and wavelengths is a three-port filter, which allows some of the wavelengths to pass through and reflects the rest. A three-port optical wavelength

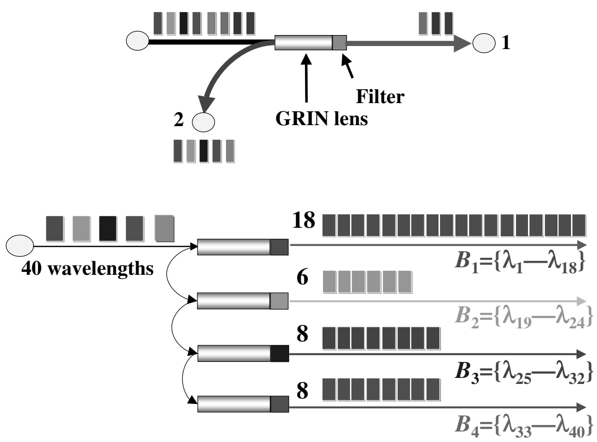

Fig. 6. Three-port filters and waveband deaggregators.

selective component is shown in the upper part of Figure 6. The component consists of three optical fibers, a self-focused GRIN lens, and a thin-film interference filter. The upper part of Figure 6 shows wavelength band separation, where a wideband DWDM filter passes a band of three wavelengths to output fiber 1 and reflects all others back into output fiber 2.

Three-port filters can be aggregated into a multi-stage system (waveband deaggregator), which delivers the desired waveband/wavelength separation. The architecture of the waveband deaggregator is essentially a cascade of (non-uniform) bandpass operations and recombinations, as illustrated in the lower part of Figure 6 (where the incoming set of 40 wavelengths is being separated into four fixed wavebands $B_1, \ldots, B_4$ containing 18, 6, 8 and 8 wavelengths respectively). The waveband sizes are thus determined by the bandpass operations.

Traditional wavelength-division multiplexers and demultiplexers (also called WDM MUXs and WDM DEMUXs) are the subsystems that combine (couple) and separate (split) different optical wavelengths. A WDM DEMUX separates the wavelength band on an incoming fiber into a number of wavelength subsets. These wavelength subsets can be uniform or non-uniform fixed groups (wavebands), as shown in Figure 6. A DEMUX subsystem may produce both fixed and arbitrary wavelength subsets. Non-uniform waveband deaggregators can be used instead of DEMUX in hybrid hierarchical optical cross-connects (shown in Figure 1), further reducing the cost of the optical node by employing a flexible set of wavebands containing different number of wavelengths.

As we already showed in Figure 6, wavebands can be created by a cascade of three-port filters. Not all the waveband sizes that are produced by our WCC algorithm can be cost efficient for our three-port filters. For example, it may be significantly cheaper to employ filters creating the wavebands of size 8 than use filters creating the wavebands of size 7. In general, the waveband sizes may have to be chosen from a set $D = \{d_1, d_2, d_3, \ldots d_n\}$, where we further assume that $d_1 \leq \ldots \leq d_n$. For example, cost considerations may make all waveband sizes but $\{1, 2, 4, 6, 8, 10\}$ impractical. In such cases, the original Waveband Cover Construction algorithm can be modified by changing step 3 in the following manner:

Algorithm 3. Modified Waveband Cover Construction (MWCC).

3) Assign $N' = \lceil N/M \rceil$. If $N' \notin D$, choose the largest element $d_i \in D$ that is smaller than N' and assign $N' = d_i$.

The above algorithm still produces a valid optimal cover that can be verified similarly to the proof of Theorem 1. The Waveband Cover Assignment algorithm remains unchanged, as can be shown from Theorem 2.

V. Performance of Switching Nodes with Non-uniform Wavebands

In order to compare the performance of non-uniform wavebands versus that of uniform wavebands, we consider a switch with a single input port receiving N wavelengths that are switched to M output ports. In this model, input wavelengths that are aggregated into wavebands are switched optically in OOO. A valid aggregation of L wavelengths into a waveband has to meet the following two conditions.

1) There exists an unused waveband of size L.
2) All L wavelengths are switched to the same output ports.

We denote the number of input wavelengths to the hierarchical node by N. We also denote the number of wavelengths that can be aggregated into wavebands and switched in OOO by P. The switching throughput S is then defined as P/N. The switching throughput thus refers to the ratio of the wavelengths that can be transparently switched to the total number of input wavelengths. The switching throughput is the key component of the aggregation benefit: if more traffic can be switched transparently, the number of expensive OEO ports can be reduced.

For a more detailed analysis of the effect of switching throughput, we consider a single node with different numbers of output ports (4, 6, and 8) serving an input fiber with 40 input wavelengths. The input wavelengths are randomly switched to the output ports based on two different traffic patterns: uniform (as in [19]) and Zipf. In the case of uniform traffic pattern, any wavelength at the input port has the same probability to be switched into any of the output ports. In the case of Zipf traffic pattern, the probability of a wavelength to be switched to a given output port is based on the weight associated with the port; the weights are selected in a way that fits a Zipf distribution. To make a fair and realistic comparison of uniform and non-uniform wavebands, we analyze sets of uniform and non-uniform wavebands containing the same number K of elements. In the case of uniform wavebands of size G, the switching throughput is calculated in the following way. Let b_i denote the number of wavelengths to be switched to the i^{th} output port. The number

number of wavebands	wavebands											switching throughput
4 output ports												
K=4	NU	13	9	9	9							60.90%
	U	10	10	10	10							55.75%
K=5	NU	9	9	9	7	6						81.10%
	U	8	8	8	8	8						67.60%
K=8	NU	10	7	7	5	4	3	2	2			95.70%
	U	5	5	5	5	5	5	5	5			80.45%
K=10	NU	10	8	5	5	4	3	2	1	1	1	99.90%
	U	4	4	4	4	4	4	4	4	4	4	84.20%
6 output ports												
K=4	NU	15	9	8	8							36.98%
	U	10	10	10	10							17.78%
K=5	NU	9	9	8	8	6						59.93%
	U	8	8	8	8	8						42.28%
K=8	NU	7	7	6	6	5	4	3	2			90.00%
	U	5	5	5	5	5	5	5	5			70.97%
K=10	NU	8	7	6	6	4	3	2	2	1	1	94.90%
	U	4	4	4	4	4	4	4	4	4	4	77.60%
8 output ports												
K=4	NU	14	14	6	6							30.00%
	U	10	10	10	10							4.70%
K=5	NU	14	8	6	6	6						42.00%
	U	8	8	8	8	8						18.07%
K=8	NU	7	7	6	5	5	4	3	3			83.70%
	U	5	5	5	5	5	5	5	5			59.25%
K=10	NU	7	6	5	5	4	4	3	3	2	1	90.70%
	U	4	4	4	4	4	4	4	4	4	4	69.93%

Fig. 7. Switching throughput for uniform traffic.

number of wavebands	wavebands											switching throughput
4 output ports												
K=4	NU	15	10	9	6							76.25%
	U	10	10	10	10							62.50%
K=5	NU	11	10	9	6	4						100.00%
	U	8	8	8	8	8						63.00%
K=8	NU	9	9	9	6	4	1	1	1			100.00%
	U	5	5	5	5	5	5	5	5			81.25%
K=10	NU	9	9	9	6	2	1	1	1	1	1	100.00%
	U	4	4	4	4	4	4	4	4	4	4	90.00%
6 output ports												
K=4	NU	15	12	8	5							25.00%
	U	10	10	10	10							17.78%
K=5	NU	12	8	8	7	5						82.50%
	U	8	8	8	8	8						35.24%
K=8	NU	9	8	8	5	3	3	2	2			100.00%
	U	5	5	5	5	5	5	5	5			75.00%
K=10	NU	9	8	8	5	3	3	1	1	1	1	100.00%
	U	4	4	4	4	4	4	4	4	4	4	80.00%
8 output ports												
K=4	NU	15	12	7	6							21.00%
	U	10	10	10	10							4.70%
K=5	NU	15	8	7	6	4						80.00%
	U	8	8	8	8	8						30.00%
K=8	NU	12	7	7	4	3	3	2	2			93.75%
	U	5	5	5	5	5	5	5	5			62.50%
K=10	NU	8	7	7	5	4	3	2	2	1	1	100.00%
	U	4	4	4	4	4	4	4	4	4	4	65.00%

Fig. 8. Switching throughput for Zipf traffic.

P of wavelengths that can be aggregated into wavebands is given by the formula $P = N - (b_1 + \ldots + b_m) \bmod G$ and determines the switching throughput $S = P/N$. In the case of non-uniform wavebands of sizes $g_1, \ldots, g_K$, we aggregate the wavelengths into wavebands using the descending order best-first-fit packing algorithm. In this algorithm, the waveband sizes g_i and numbers b_i of wavelengths to be switched in the corresponding output ports i, are first sorted in descending order. Subsequently, we aggregate wavelengths into wavebands using the following packing algorithm:

Algorithm 4. Waveband Packing (WP).
For each g_i, where $i = 1, 2, \ldots, k$:

1) Let $b_{\max}$ be the maximum over all numbers b_i
2) If $b_{\max} \geq g_i$ then
   Aggregate g_i wavelengths out of $b_{\max}$
   Assign $b_{\max} = b_{\max} - g_i$.

As a result of the WP algorithm, the switching throughput is given by $S = P/N$, where $P = b_1 + \ldots + b_m$. For each set of parameters, 300 different input-to-output ports switching combinations are generated, based on the corresponding traffic pattern (uniform or Zipf). The resulting throughput is obtained by averaging the simulated switching combinations.

The results for uniform traffic distribution are shown in Figure 7. They demonstrate that non-uniform wavebands consistently deliver superior switching throughput, which translates into a significant increase in aggregation benefits of the hierarchical optical switching. As the number of wavebands increases, the switching throughput for both uniform and non-uniform wavebands also increases. However, the difference between their throughput is larger when higher number of wavebands are used. For example, with 4 output ports, at $k = 4$, the difference between the throughputs is 5.15% whereas at $k = 10$, the difference is 15.7%. As the number of output ports increases, the switching throughput decreases since the routing of wavelengths becomes more diverse (wavelength divergence) and less suitable for aggregation. For example, consider $M = 4$ and $M = 8$ with $k = 10$. In this case, the difference between the throughputs is 15.7% for $M = 4$, while it is 20.77% for $M = 8$. This example illustrates that non-uniform wavebands can handle wavelength divergence in a more efficient manner than uniform wavebands.

The results for Zipf traffic distribution are shown in Figure 8 and are similar to those obtained for uniform traffic distribution. In general, the switching throughput under the more realistic Zipf traffic distribution is higher than the one obtained for uniform traffic distribution.

VI. Non-Uniform Wavebands in Ring Networks

In this section, we consider the Waveband Cover Assignment algorithm in the case of a single hub metropolitan ring topology. Specifically, we consider the ring network that is used as an access network, where all the traffic is from the access nodes in the ring to the hub. Our objective here is to aggregate the lightpaths from access nodes to the hub into wavebands, in a way that minimizes the overall port costs. We assume that a lightpath from a node to the hub can follow either clockwise or anti-clockwise direction, depending on wavelength availability. Given the traffic demand from all access nodes and the corresponding routes, we perform the following waveband aggregation.

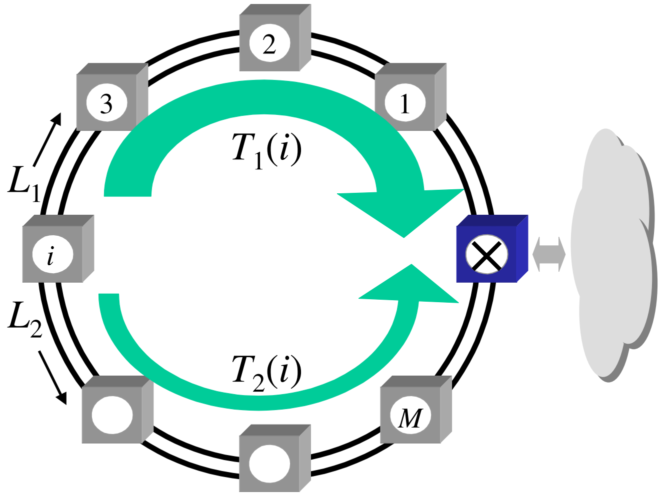

Fig. 9. Simulated optical ring topology.

***M*=40**
Uniform wavebands (53):
3 3 3 3 3 3 3 3 3 3 3 3 3 3 3 3 3 3 3 3 3 3 3 3 3 3 3 3
3 3 3 3 3 3 3 3 3 3 3 3 3 3 3 3 3 3 3 3 3 3 3 3 3
Non-uniform wavebands (53):
8 8 8 7 7 7 6 6 6 5 5 5 5 4 4 4 4 4 3 3 3 3 3 3 2 2 2 2
2 2 2 2 2 2 1 1 1 1 1 1 1 1 1 1 1 1 1 1 1 1 1 1 1

***M*=30**
Uniform wavebands (40):
4 4 4 4 4 4 4 4 4 4 4 4 4 4 4 4 4 4 4 4
4 4 4 4 4 4 4 4 4 4 4 4 4 4 4 4 4 4 4 4
Non-uniform wavebands (44):
11 10 10 9 8 8 7 7 6 6 6 5 5 5 4 4 4 3 3 3 3
3 2 2 2 2 2 2 2 2 1 1 1 1 1 1 1 1 1 1 1 1 1 1

***M*=20**
Uniform wavebands (32):
5 5 5 5 5 5 5 5 5 5 5 5 5 5 5 5 5 5 5 5 5 5 5 5 5 5 5 5 5 5 5 5
Non-uniform wavebands (33):
16 15 13 12 11 10 9 8 7 6 6 5 5 4 4 3 3 3 2 2 2 2 2 1 1 1 1 1 1 1 1 1 1

***M*=10**
Uniform wavebands (20):
8 8 8 8 8 8 8 8 8 8 8 8 8 8 8 8 8 8 8 8
Non-uniform wavebands (19):
32 26 21 17 13 11 8 7 5 4 4 3 2 2 1 1 1 1 1

Fig. 10. Comparable sets of uniform and non-uniform wavebands.

Consider a ring with M access nodes and a single hub. For each access node, let L_1 and L_2 be the two incoming and outgoing links (all links are assumed to be able to accommodate $N = 160$ wavelengths), in the clockwise and counterclockwise directions, respectively (Figure 9). For a given access node i we denote by $T_1(i)$ the traffic load (number of wavelengths) from node i to the hub using the link L_1; similarly, we define $T_2(i)$ as shown in Figure 9. As a result, we have two sets (clockwise and counter-clockwise) of traffic flows denoted by $S_j = \{T_j(i) | i = 1, \ldots, M\}$, for $j = 1, 2$ (shown in Figure 9). We next consider the waveband aggregation for each of the two S_j. Denote by D the number of all wavelengths for a given set S_j; in other words, $D = T_j(1) + \ldots + T_j(M)$.

If $D = N$, the problem of aggregating N wavelengths converging to a single hub from M access points is similar to the problem of arbitrarily breaking down N wavelengths into M ports. Therefore, we can construct a pre-configured set of wavebands B (as discussed in Section III) to cover any breakdown of wavelengths. Given the set of wavebands B, we can assign the wavebands to each traffic flow $T_j(i)$, for $i = 1, \ldots, N$, using the WCA algorithm described in Section III. We follow the same methods for aggregation in the case of the other set S_j. Because of the way of band construction and assignment, it is ensured that each traffic wavelength path is aggregated into a waveband that originates at the corresponding access node and extends to the hub node. As a result, the only OEO ports used are those at the source (access) nodes for add/drop purpose; the remainder of the paths are completely in the optical domain.

If $D < N$, the problem is slightly modified in the following way. We assign imaginary traffic load $R = N - D$ from the node closest to the hub. The problem then becomes the same as the one analyzed in the previous paragraph and can be solved in the same way. For computing the overall performance, we exclude the wavebands that are assigned to the imaginary traffic from cost computation.

We simulated the performance of the proposed approach on four rings of different sizes (M=10,20,30 and 40). The port cost is discussed in section II.B. For simplicity, we assumed the traffic is routed along the shortest path to the hub node.

For each of the four rings, we simulated multiple instances of traffic matrices by assuming that each node sends to the hub node a random number of wavelengths. Two types of traffic distributions were simulated, referred to as uniform (where the random number of wavelengths is uniformly distributed in an appropriately selected segment) and Zipf (where the random number of wavelengths is generated by Zipf distribution). Different traffic loads were simulated as well, ranging from 20% to 90% (the load was defined as the average occupancy of bottleneck links to the hub node).

We compared the performance of non-uniform wavebands with that of uniform wavebands. For a fair comparison, the size of uniform wavebands was selected so that the total number of uniform wavebands be close to that of non-uniform wavebands. Note that it is not always possible to make the numbers of elements in both sets of wavebands to be the same, since the total number of wavelengths (40) may not be divisible by the number of elements in the set of non-uniform wavebands. Figure 10 shows uniform and non-uniform wavebands that were simulated for our four rings.

Our simulation results are shown in Figures 11 and 12. These figures show the cost benefit (relative cost reduction, as compared to the uniform wavebands) that can be achieved using non-uniform wavebands. For all simulated scenarios (ring sizes, loads and traffic distributions), the cost benefit provided by non-uniform wavebands is consistently within the range 25%-30%. This cost benefit is smaller than the average value observed in Section V. The node-level benefit of non-uniform wavebands demonstrated in Section V becomes smaller in network-level scenarios due to relative aggregation efficiency of ring networks observed in [7]. As a result of this efficiency (there is little routing diversity in ring networks),

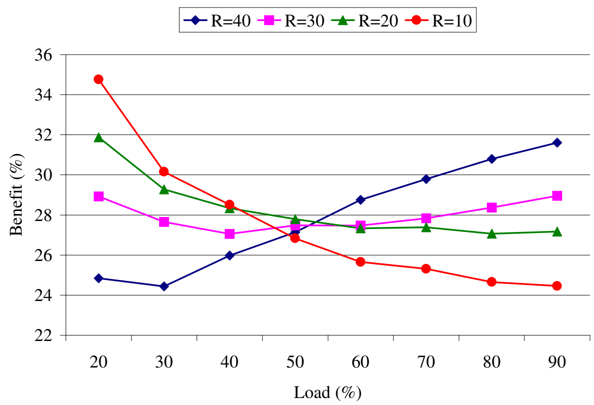

Fig. 11. Ring networks: aggregation cost benefit for uniform traffic distribution.

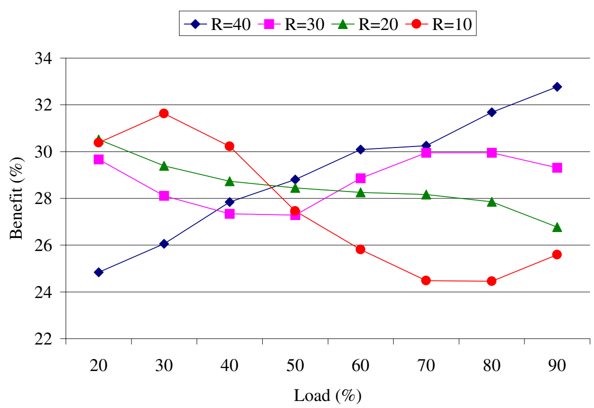

Fig. 12. Ring networks: aggregation cost benefit for Zipf traffic distribution.

uniform waveband aggregation performs sufficiently well, so the additional performance improvement provided by non-uniform wavebands is relatively smaller.

VII. Non-Uniform Wavebands in Mesh Networks

In the previous section, we used non-uniform wavebands to aggregate wavelength flows from the access nodes to the hub. The same approach can be also applied with a few modifications to the case of a general mesh topology . Let us consider a specific node i that receives non-zero wavelength flows from a number $M(i)$ of sources. The wavelength path for each flow connects the node i through one of its incidence links. We denote by $N(i)$ the maximum number of wavelengths paths that use any of the incidence links of node i.

Using these definitions, we can find $N_{\max} = \max_i[N(i)], \forall i$ and $M_{\max} = \max_i[M(i)]$. We use our WCC algorithm with $N = N_{\max}$ and $M = M_{\max}$ to find the optimal set of non-uniform wavebands to be used in the hybrid nodes of the mesh network.

Since the waveband cover construction is obtained for the worst case scenario, we can always use one or more wavebands to aggregate traffic from all sources to the single destination, by following our Waveband Cover Assignment algorithm, as we did in the case of a ring network. This strategy will not work with multiple destinations for the following reason. Consider two nodes i and j receiving traffic flows from a source s and assume that the wavelength paths for these flows share a common link. There might arise a case where the same waveband needs to be assigned to traffic from $s \rightarrow i$ and $s \rightarrow j$, something that will make the waveband assignment infeasible.

We can deal with this case if we assume that wavebands do not have to be completely filled: a waveband of size G does not necessarily have to have exactly G active wavelengths. The assumption of incomplete wavebands is a natural step in network evolution: by provisioning incomplete wavebands, the benefits of all-optical layer can be obtained from the start, while the wavebands can be filled as the traffic load increases. Under this assumption, we can modify our WCA algorithm that assigns the maximum size waveband that is available in the entire path from source to destination. The formal description is as follows.

First, we create the set of wavebands B using our WCC algorithm. Next, for any undirected link l of the network, we denote by $A(l)$ the set of available wavebands in the link. Initially, $A(l) = B$ for all links in the network. Let $T[i, j]$ denote the total number of wavelengths used by the traffic flow from node i to node j. We next perform the following steps for assignment.

Algorithm 5. Waveband Assignment in Mesh Networks (WAM).

1) Find $i_{\max}, j_{\max}$ for which $T[i, j]$ is the maximum.
2) If $T[i_{\max}, j_{\max}] <= 0$ stop; else goto step 3.
3) Let L be the set of links from $i_{\max} \rightarrow j_{\max}$.
4) Find the largest waveband size $B_{\max}$ available in all links in L.
5) Assign $B_{\max}$ to traffic from $i_{\max} \rightarrow j_{\max}$.
6) Update $T[i_{\max}, j_{\max}] = T[i_{\max}, j_{\max}] - B_{\max}$.
7) Exclude the waveband $B_{\max}$ from all links in L.
8) Goto step 1.

We simulated the WAM algorithm in a general US network (shown in Figure 13) with relative traffic distribution proportional to the population in the source nodes. Four scaled versions of the traffic distribution were simulated (matching the doubling of traffic volume every year). The port cost using wavebands is discussed in section II.B.

We further compared the cost benefits that could be obtained by replacing OEO cross-connects with hybrid hierarchical nodes with both uniform and non-uniform wavebands. The results are shown in Figure 14.

In consistency with the previous sections, the results illustrate the competitive cost reduction provided by non-uniform wavebands under different traffic load conditions. In particular, the advantage becomes greater as the traffic load increases.

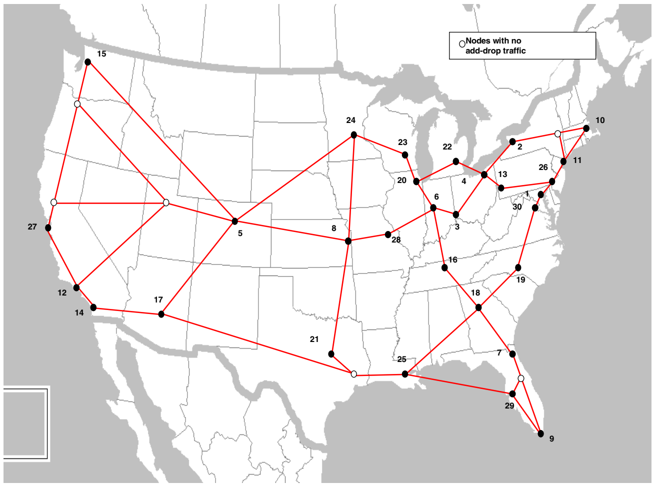

Fig. 13. Simulated mesh network topology.

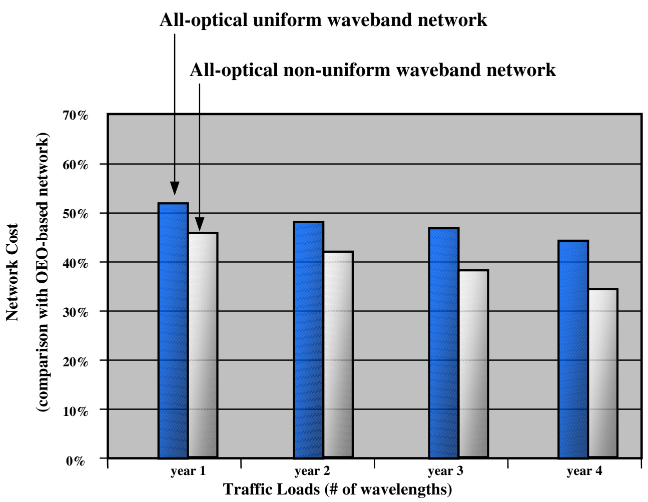

Fig. 14. Mesh network: aggregation cost benefit for uniform and non-uniform wavebands.

VIII. Conclusion

We presented a formal model for describing the effect of waveband aggregation in a single optical node. For this model, we formulated two complementary problems and provided an optimal algorithmic solution for both of them. We analyzed the switching performance of non-uniform wavebands for the case of a single node. Further, we applied the concept of non-uniform wavebands to aggregate wavelength traffic in the case of metro-access ring and mesh network. Detailed simulation results showed significant cost reduction in the case of both ring and mesh network by using non-uniform wavebands rather than uniform wavebands.

Our future plans involve exploring the wavelength and waveband routing problem in general network topology with the goal of minimizing the port cost. The wavelength continuity constraints and assignment restrictions add further challenge to the waveband selection and assignment problem. We plan to incorporate these constraints while investigating the wavelength and waveband assignment problem in both offline and online traffic scenarios.

Acknowledgement

Authors are grateful to L.French (Semandex, Inc.) for fruitful discussions.

References

[1] R. Ramaswami, and K.N. Sivarajan, K. N., *Optical Networks: A Practical Perspective,* Morgan Kaufmann Publishers, 1998.

[2] K. Kilkki, *Differentiated Services for the Internet,* Macmillan Publishing, June 1999.

[3] B. Davie and Y. Rekhter, *MPLS: Technology and Applications,* Morgan Kaufmann Publishers, 2000.

[4] L. Noirie, M. Vigoreux, E. Dotaro, "Impact of intermediate trafic grouping on the dimensioning of multi-granularity optical networks", *Proceedings of OFC 2001*.

[5] R. Lingampalli and P. Vengalam, "Effect of wavelength and waveband grooming on an all-optical networks with single layer photonic switching," *Proceedings of OFC 2002*.

[6] Y. Suemura, I. Nishioka, Y. Maeno and S. Araki, "Routing of hierarchical paths in an optical network", *Proceedings of APCC 2001*.

[7] Y. Suemura, I. Nishioka, Y. Maeno, S. Araki, R. Izmailov, S. Ganguly "Hierarchical routing in layered ring and mesh optical networks", *Proceedings of IEEE ICC 2001*.

[8] S. Araki, S. Ganguly, R. Izmailov, Y. Maeno, Y. Suemura, T. Wang, "Hybrid cross-connects and hierarhical optical networks", *NEC R&D Journal* Vol. 43, No. 2, pp. 133-140, April 2002.

[9] R. Izmailov, S. Ganguly, T. Wang, Y. Suemura, Y. Maeno, S. Araki, " Hybrid hierarchical optical networks", *IEEE Communications Magazine*, Vol. 40, No. 11, pp. 88-95, Nov. 2002.

[10] S. Ganguly, R. Izmailov, T. Wang, S. Araki, Y. Maeno, "Non-uniform wavebands and hierarchical optical networks", *Proceedings of NFOEC 2002*.

[11] M. Lee, J. Yu, Y. Kim, C.-H. Kang, and J. Park, "Design of hierarchical crossconnect WDM networks employing a two-stage multiplexing scheme of waveband and wavelength," *IEEE Journal on Selected Areas in Communications*, Vol. 20, pp. 166-171, No. 1, 2002.

[12] R. Izmailov, A. Kolarov, R. Fan and S. Araki, "Hierarchical optical switching: a node-level analysis," *Proceedings of IEEE Workshop on High Performance Switching and Routing 2002*.

[13] O. Gerstel, R. Ramaswami, and S.Foster, "Merits of hybrid optical networking," *Proceedings of OFC 2002*.

[14] E. Ciaramella, "Introducing wavelength granularity to reduce the complexity of optical cross connects," *IEEE Photonic Technology Letters*, Vol. 12, pp. 699-701, No.6, June 2000.

[15] P. Ho and H. Mouftah, "Path selection with tunnel allocation in the optical internet based on generalized MPLS architecture," *Proceedings of IEEE GLOBECOM 2001*.

[16] S. Martello and P. Toth, *Knapsack Problems: Algorithms and Computer Implementations*, John Wiley, New York, 1990.

[17] B. Patt-Shamir, Y. Tsiounis, Y. Frankel, "Exact analysis of exact change: the k-payment problem", SIAM Journal on Discrete Mathematics, 2002, Vol. 13, No. 4, pp. 436-453.

[18] G. Andrews, *The Theory of Partitions*, Encyclopedia of Mathematics and its Applications, Vol. 2, Addison-Wesley Publishing Co., Reading, Mass.-London-Amsterdam, 1976.

[19] R. Izmailov, S. Ganguly, T. Wang, S. Araki, Y. Maeno, "Switcing performance of non-uniform wavebands in hierarchical optical networks", *Proceedings of OECC 2002*.